Am J Transl Res 2020;12(11):7297-7311
www.ajtr.org /ISSN:1943-8141/AJTR0108013

Original Article

WISP1 indicates poor prognosis and regulates cell proliferation and apoptosis in gastric cancer via targeting AKT/mTOR signaling pathway

Yanyan Zhu, Wei Li, Yuanyuan Yang, You Li, Yueyue Zhao

Department of Pediatrics, The First Affiliated Hospital of China Medical University, Shenyang 110001, China

Received January 17, 2020; Accepted October 11, 2020; Epub November 15, 2020; Published November 30, 2020

Abstract: Purpose: Gastric cancer (GC) is a serious threat to human health. We aimed to explore the effects of Wnt1 induced signaling protein 1 (WISP1) on GC. Methods: The WISP1 expressions in GC tissues were detected using immunohistochemistry and qRT-PCR. The connection between GC prognosis and WISP1 expression was analyzed via Pearson's χ^2 test. The WISP1 expressions were down-regulated in GC cells through siWISP1 transfection. Colony formation assay and cell counting kit-8 assay were carried out to measure cell colony formation and proliferation, respectively. Flow cytometry was operated to examine the cell cycle and apoptosis. The protein expressions in our study were assessed using western blot. The AKT pathway was blocked by LY294002 treatment and then the cell activities were assessed. Furthermore, GC mice models were established to investigate the effects of WISP1 on GC *in vivo*. Results: We found that WISP1 was highly expressed in GC cells and tissues. The up-regulation of WISP1 was related to poor prognosis of GC patients. WISP1 down-regulation reduced colony formation and cell proliferation, resulted cell cycle arrest and promoted cell apoptosis in GC. WISP1 knockdown suppressed AKT/mTOR pathway activity. LY294002 treatment recovered the decreases of colony formation and cell proliferation, arrest of cell cycle and increase of cell apoptosis which were induced by WISP1 knockdown. WISP1 down-regulation repressed GC tumor growth and enhanced tumor apoptosis *in vivo*. Conclusion: WISP1 regulated GC cell proliferation and apoptosis *in vivo* and *in vitro* through activating AKT/mTOR pathway. WISP1 might be a target in GC therapy.

Keywords: Gastric cancer, WISP1, AKT, mTOR, proliferation

Introduction

Gastric cancer (GC) is the third deadliest cancer in the world, and the second deadliest cancer in the digestive tract [1]. In the past 50 years, the incidence of GC in the world was declined significantly, which was closely related to the progress of sanitation, clean water supply and food preservation [2, 3]. However, GC is still a global health problem. Worldwide, more than 1 million new cases of GC were diagnosed in 2018, and an estimated 783,000 people died of the disease [1]. The related clinical statistical results show that the incidence and death rate of GC in China account for about 50% of the total number of people in the world, and the death rate of male patients with GC is twice that of female patients [4].

In the early stage of GC, there are no obvious symptoms. The first non-specific symptoms are latent, such as abdominal discomfort, dull pain and weight loss. They are very similar to those of chronic gastritis and chronic gastric ulcer [5]. These symptoms are easy to be ignored by patients and delay diagnosis and treatment. Moreover, there is no specific clinical, imaging, or even pathological manifestations in the early stage of GC [6]. Therefore, early detection rate of GC is still unfavorable. Most of the patients with GC were in advanced stage when they were admitted to the hospital and were accompanied by lymphatic metastasis or distant tissue and organ diffusion metastasis, resulting in low treatment success rate, low surgical survival rate and high 5-year mortality [7]. Therefore, early diagnosis of GC and searching for prognostic biomarkers are of great clinical significance. In recent years, with the in-depth study of the molecular mechanism of GC, a series of molecular targeted biomarkers have been found and gradually used in clinical treatment [8], such as microRNA-130a (miR-130a) [9], erythrocyte membrane protein band 4.1-like 5

(EPB41L5) [10] and long non-coding RNA HOXA transcript at the distal tip (LncRNA HOTTIP) [11]. However, the understanding of biomarkers in GC remains to be deepened.

Wnt1 induced signaling protein 1 (WISP1), also known as CCN4, is located on human chromosome 8p24.1-8p24.3 with molecular weight of 40 KDa [12]. WISP1, as a cellular matrix protein, is involved in a variety of cellular processes, including cell differentiation, proliferation, metastasis and survival [13]. Mouse WISP1 homologues were first identified, and the expression of WISP1 homologues in high and low metastatic cells was significantly different [14]. WISP1 was proved to regulate a number of pathophysiological processes including inflammation, wound repair, angiogenesis, and fibrosis [15, 16]. WISP1 has been reported to exert significant abnormal expressions during the occurrence and development in some tumors, such as prostate cancer [17], laryngeal cancer [18] and breast cancer [19]. However, its role in GC is unclear.

In the present study, we found that WISP1 was over-expressed in GC tumor tissues and cell lines. And, the high expression of WISP1 indicated the poor prognosis of GC patients. We confirmed that the knockdown of WISP1 inhibited GC cell proliferation and promoted cell apoptosis *in vitro* and *in vivo* by regulating protein kinase B/mechanistic target of rapamycin (AKT/mTOR) signaling pathway. Our findings might provide a novel biomarker for the diagnosis, prognosis and accurate treatment of GC patients.

Materials and methods

The Cancer Genome Atlas (TCGA) analysis

The expressions of WISP1 in 415 cases of GC tumor tissues samples and in 34 cases of normal samples were downloaded from the TCGA database (https://portal.gdc.cancer.gov/). The expression levels of WSIP1 in all of the above GC tissues and non-tumor normal tissues were assessed and compared. In addition, the data of the effect of WISP1 expression level on GC patient survival rates was also harvested from TCGA database.

GC tumor tissues

GC patients (n = 69) were enrolled in our research, and these patients were not subjected with radiotherapy or preoperative neoadjuvant chemotherapy. The 69 paired of GC tumor tissues and adjacent non-tumor tissues were collected from January 2010 to December 2013 at the First Affiliated Hospital of China Medical University after these GC patients underwent radical gastrectomy. This study was approved by the Clinical Research Ethics Committee of the First Affiliated Hospital of China Medical University. The median WISP1 expression level in 69 cases of GC tissues were analyzed using Kaplan-Meier survival analysis through SPSS 18.0 (IBM, USA) and then acted as truncation value. The GC tumor samples with WISP1 expression higher than the median were classified as WISP1 high expression group, while the samples with WISP1 expression lower than the median were classified as WISP1 low expression group.

Cell lines

Human GC cell lines (MKN45, MKN28, HGC-27, SGC7901 and BGC823) and normal gastric mucosal epithelial cell (GES-1) were purchased from the Type Culture Collection of the Chinese Academy of Sciences (Shanghai, China). Dulbecco's Modified Eagle's Medium high glucose medium (DMEM), containing 10% fetal bovine serum (FBS), 100 U/mL penicillin and 100 μg/mL streptomycin, was obtained from Gibco (Grand Island, NY, USA). And, it was then applied to incubate these cell lines in an incubator at room temperature with 5% CO_2.

Cell transfection

Small interfering WISP1 (siWISP1) plasmid, small interfering negative control (siNC) plasmid, short hairpin WISP1 (shWISP1) plasmid and short hairpin negative control (shNC) plasmid were all commercially designed and purchased from Genechem (Shanghai, China). Lipofectamine 3000 that bought from Invitrogen (Carlsbad, CA, USA) was used to transfect above plasmids into human GC cell lines SGC7901 and/or BGC823 with the accordance of manufacturer's instructions.

Quantitative real-time polymerase chain reaction (qRT-PCR)

TRIzol® reagent, purchased from Invitrogen, was employed to separate the total RNA essentially according to the manufacturer's protocol. The First Strand cDNA Synthesis kit, oligo primers (dT) and RNA (1 μg), provided by Thermo

Scientific (Waltham, MA, USA), were applied to operate RT-PCR reactions at 42°C for 1 h to harvest cDNA. The KAPA SYBR® FAST kit, provided by Sigma Aldrich (San Luis, MO, USA) and specific primers were used to perform qRT-PCR. The qRT-PCR was carried out in a Stratagene Mx3000P real-time thermal cycler with the cycling conditions as follow: one cycle at 95°C for 10 min, followed by 40 cycles at 95°C for 15 s, 60°C for 15 s, 72°C for 20 s, and a final cycle at 95°C for 1 min. The results were analyzed with the A MxPro Qpcr software, obtained from Agilent Technologies (Santa Clara, CA, USA), was proceeded to analyzed the qRT-PCR data and the data were then calculated through the $2^{-\Delta\Delta Ct}$ method. β-actin was acted as the normalized gene. The specific primers used in our paper were as follows: WISP1: 5'-CAGCACACGCTCCTATCA-3' and 5'-CAAGCCCATCAGGACACT-3'; β-actin: 5'-GCTCGTCGTCGACAACGGCTC-3' and 5'-CAAACATGATCTGGGTCATCTTCTC-3'.

Immunohistochemistry (IHC) assay

IHC was carried out to explore the expressions of WISP1 and Ki-67 in GC tumor tissues and normal tissues. Paraffin-embedded tissue sections (5 μm/section) thick were deparaffinized with xylene, and then rehydration with a graded series of ethanol (100%, 90%, 80% and 70%). After washing with phosphate-buffered saline (PBS), H_2O_2 (0.3%) was applied to deactivate the intrinsic peroxidase. Skim milk was then used to block the intrinsic biotin, and the primary antibodies (WISP1 antibody and Ki-67 antibody) were employed to react with the sections. After washing, secondary antibody was subsequently used to treat the sections, and H_2O_2 was supplemented to 3,3'-diaminobenzidine tetrahydrochloride (DAB) to proceed reaction. Then, methyl green was used to stain the sections, and the expression of target proteins were photographed under a light microscope (×100, ×200 and ×400, Olympus, Tokyo, Japan).

Cell counting kit-8 (CCK-8) assay

Cell proliferation was detected by CCK-8 assay in our study. At 24 h after transfection, BGC823 and SGC7901 cells were collected and then the single cell suspensions were prepared via Eagle's minimum essential medium (EMEM) at a dose of 4×10^4 cells/mL. Then, the cells were subsequently implanted in a 96-well plate at a dose of 0.1 mL/well under aforementioned conditions. A CCK-8 solution, bought from Sigma-Aldrich (Merck KGaA), was supplemented to each well at 0 h, 24 h, 48 h and 72 h. The optical density (OD) values were detected at 450 nm by a microplate spectrophotometer (Thermo Labsystems, Vantaa, Finland).

Colony formation assay

A RPMI-1640 medium was used to re-suspend the cells and then petri dishes (35 mm) were used to plate them at 37°C. The cells were then washed with PBS and fixed with 4% paraformaldehyde for 20 min. Then, a Wright-Giemsa solution, purchased from Jiancheng Bioengineering Institute (Nanjing, China), was used to stain the cell lines for 5 min. The numbers of colony cell were counted and imaged under a light microscope (Olympus, Tokyo, Japan).

Flow cytometry

For cell cycle analysis, the GC cells were collected (550×g, 5 min) and fixed with ethanol at 4°C for 2 h. Then, a total of 25 μL propidium iodide (PI, Beyotime, Haimen, China) was used to stain the ethanol-fixed cells at 37°C for 30 min. BD flow cytometer, which was purchased from Franklin Lakes (NJ, USA), was performed to measure the cell cycle distribution. For cell apoptosis analysis, the cell lines in our study was centrifuged at 309×g for 5 min, and then washed with PBS. After that, Binding buffer was used to re-suspend the cells at a density of 1×10^6 cells/mL. Then, Annexin V-FITC (5 μL, Thermo) and PI (10 μL, Beyotime) were used to stain the cells at room temperature for 15 min. Cell apoptosis was investigated by BD flow cytometer (Franklin Lakes).

Western blot

The proteins in GC cell lines and tumor tissues were extracted with Radioimmunoprecipitation assay (RIPA, 500 μL, Thermo Fisher Scientific, Illinois, USA) buffer. Protein concentrations were determined using a BCA Protein Quantification kit that purchased from Thermo Fisher Scientific (Darmstadt, Germany) with the accordance of manufacturer's protocol. A total of 50 μg proteins were isolated through 10% sodium dodecyl sulfate-polyacrylamide gel electrophoresis (SDS-PAGE) and then transferred onto

polyvinylidene difluoride membranes. Non-fat dry milk (5%) was used to block the membranes at room temperature for 1 h specific primary antibodies were used to incubate them at 4°C overnight. The primary antibodies were all provided by Abcam (Cambridge, MA, USA) and used were as follows: anti-WISP1 (1:1000, ab-178547), anti-PCNA (1:1000, ab29), anti-Cyclin D1 (1:200, ab16663), anti-Cleaved-caspase-3 (1:1000, ab2302), anti-caspase-3 (1:500, ab-13847), anti-Bcl-2 (1:1000, ab32124), anti-Bax (1:1000, ab32503), anti-p53 (1:1000, ab26), anti-p-AKT (1:1000, ab38449), anti-AKT (1:1000, ab175354), anti-p-mTOR (1:1000, ab109268), anti-mTOR (1:2000, ab2732) and anti-β-actin (1:1000, ab8227). β-actin was acted as the normalized protein. The blots were assessed by an enhanced chemiluminescence substrate kit (Thermo Fisher) according to the manufacturer's protocol. The bands were quantified by ImageJ software (version 1.47, National Institutes of Health).

AKT signaling pathway inhibitor treatment

The BCG823 cells were treated with AKT inhibitor LY294002 (20 μM, ab120243, Abcam) to block the AKT pathway according to the manufacturer's instructions. The BCG823 cells were subsequently divided into three groups: siNC, siWISP1 and siWISP1 + LY294002 groups. Then, the cell proliferation, colony formation, cell cycle and apoptosis were detected. Each treatment was performed in triplicate.

Xenograft GC tumor model

A total of 12 BALB/c nude mice (6 weeks) were bought from Shanghai Laboratory Animal Center (Shanghai, China) and then injected with 1×10^7 BGC823 cell lines that were stably transfected with shWISP1 or shNC. The mice were divided into shWISP1 group and shNC according to the different treatments. Then, the volumes of mice were monitored weekly using the formula: volume = (length × width^2)/2. At 21 d after injection, the mice were sacrificed and the tumor tissues were harvested. The tumor size and weight were subsequently measured. In addition, the expressions of Ki-67 and WISP1 in mice tumor tissues were detected using IHC assay. And, the tumor apoptosis was determined using terminal deoxynucleotidyl transferase-mediated dUTP nick-end labeling (TUNEL) assay. The animal study was approved by the Ethics Committee of the First Affiliated Hospital of China Medical University.

TUNEL assay

The apoptotic cells in mice tumor tissues were stained using TUNEL experiment. In brief, paraformaldehyde (4%) was used to fix the samples in PBS at room temperature for 30 min and then Triton X-100 (0.2%) was used to permeabilize them for 30 min at room temperature. Next, the tissue samples were incubated with TUNEL solution (Roche Diagnostics GmbH, Mannheim, Germany) was used to incubate the tissue samples with the accordance of manufacturer's protocols. Subsequently, 4',6-diamidino-2-phenylindole (DAPI) was applied to counterstain the samples. The apoptotic cells was observed under a laser confocal microscope that provided by Leica Microsystems (TcS SP5, Buffalo Grove, IL, USA), and the percentage of TUNEL-positive cells was monitored by counting from random fields of view.

Statistical analysis

Statistical analysis was constructed using SPSS 18.0 (IBM, USA), and the data were exhibited as mean ± standard deviation (SD) of at least three independent experiments. The relationship between WISP1 and patients' survival rate were analyzed using Kaplan-Meier survival analysis. The relationship between WISP1 expression levels and GC pathological features (ages, gender, pathological stages, tumor size and lymph node metastasis) was measured using Pearson's χ^2 test. Student's t-test or one-way ANOVA were used to compare the differences among groups. Log-rank test was performed to calculate *P*-value and $P < 0.05$ presented statistically significant.

Results

WISP1 overexpressed in GC tissues

Data from TCGA database showed that WISP1 was significantly over-expressed in GC tumor tissues (n = 415) compared to that in non-tumor tissues (n = 34) ($P < 0.01$, **Figure 1A**). And, the data also elucidated that the survival probabilities of the 97 cases of WISP1 high expression patients were obviously lower than the 295 cases of WISP1 low expression patients ($P = 0.039$, **Figure 1B**). Next, the expres-

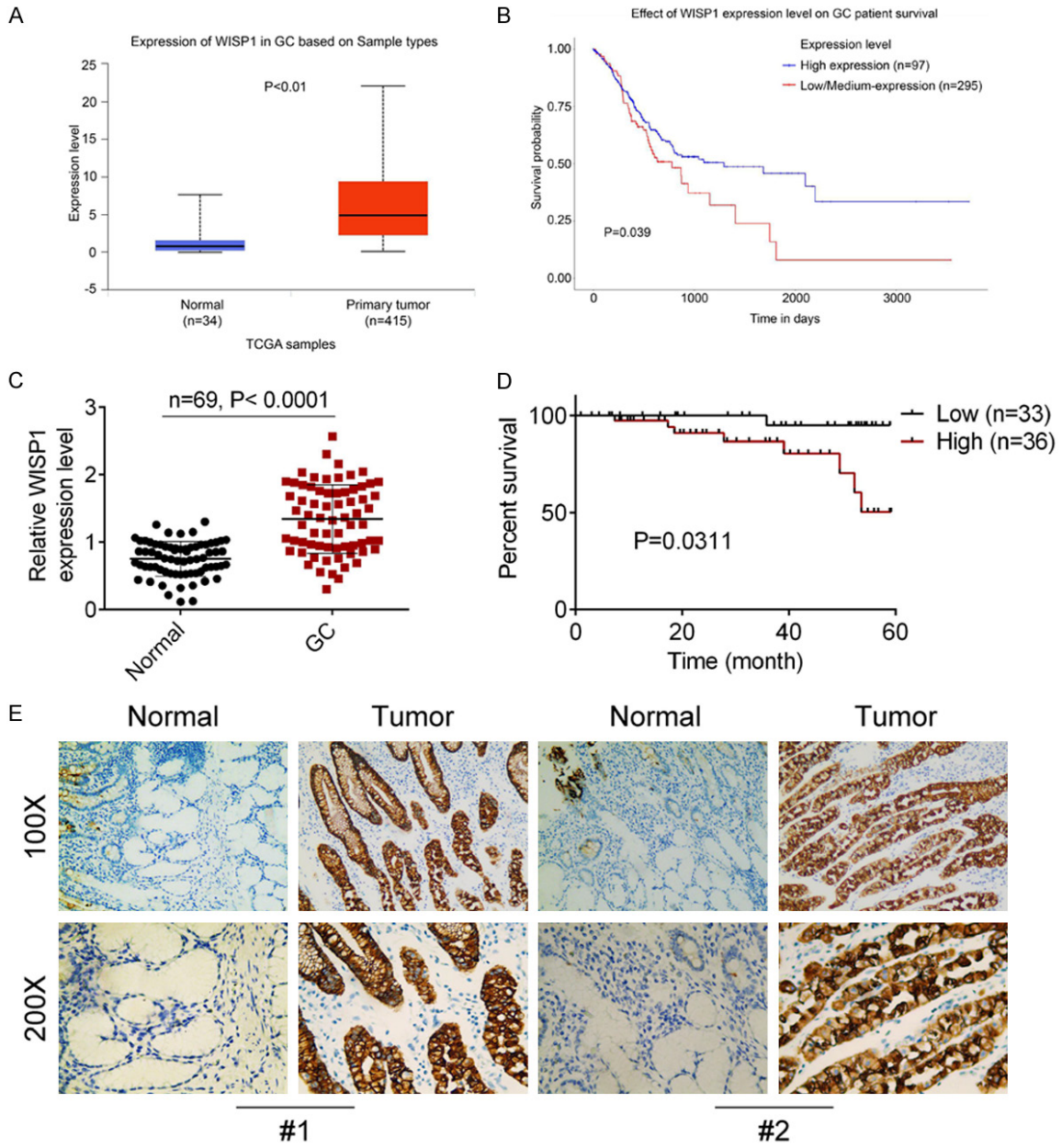

Figure 1. WISP1 was overexpressed in GC tissues. A. The data of WISP1 expressions in 415 cases of GC tumor tissues and 34 cases of adjacent non-tumor tissues were downloaded from TCGA database. B. The effects of high (n = 97) or low (n = 295) WISP1 expression on GC patient survival rates were downloaded from TCGA database. C. The expression levels of WISP1 in 69 cases of GC tumor tissues and matched normal tissues were detected using qRT-PCR. D. The 69 cases of GC tumor tissues were divided into high WISP1 expression level and low WISP1 expression level, and the relationship between WISP1 and patients' survival rate were analyzed using Kaplan-Meier survival analysis. E. The expression levels of WISP1 in 2 paired of GC tumor tissues and adjacent normal tissues were measured using IHC. Data were shown as mean ± SD.

sions of WISP1 in 69 paired of GC tumor tissues and adjacent non-tumor tissues were detected using qRT-PCR and the results revealed that WISP1 was notably highly expressed in GC tumor tissues compared to that in normal tissues ($P < 0.01$, **Figure 1C**). Then, the 69 cases of GC tumor samples were divided into WISP1 high expression group and low expression group according to the median expression level of WISP and the relationship between WISP1 expression and survival rate of patients were analyzed. As shown as **Figure 1D**,

Table 1. Correlation between WISP1 expression level and clinical features in GC

Characteristics	Number of patients	WISP1 Low expression (< median)	WISP1 High expression (≥ median)	*P* value
Number	69	33	36	
Ages (years)				0.546
< 45	35	17	18	
≥ 45	34	16	18	
Gender				0.554
Female	33	16	17	
Male	36	17	19	
Pathological stage				0.021
I-II	30	19	11	
III-IV	39	14	25	
Tumor size				0.011
< 3 cm	31	20	11	
≥ 3 cm	38	13	25	
Lymph node metastasis				0.275
Yes	34	18	16	
No	35	15	20	

the survival rate of WISP1 high expression group was remarkably lower than than of WISP1 low expression level ($P = 0.0311$). Furthermore, two pairs of GC tumor tissues and adjacent non-tumor tissues were treated with IHC assay to determine the WISP1 expressions. Similarly, the results of IHC assay also demonstrated that the WISP1 expressions in GC tumor tissues were dramatically higher than those in normal tissues ($P < 0.01$, **Figure 1E**). In addition, the relationship between WISP1 expression and GC pathological features were monitored and the results were displayed as **Table 1**. Obviously, the WISP1 expression was related to pathological stage and tumor size. These results showed that WISP1 was over-expressed in GC tissues and its over-expression indicated poor prognosis of GC patients.

Knockdown of WISP1 inhibited cell proliferation and promoted cell apoptosis in GC cell lines

The expression levels of WIPS1 in normal cell lines GES-1 and GC cell lines including MKN45, MKN28, HGC-27, BGC823 and SGC7901 were detected using qRT-PCR and western blot. Data from qRT-PCR and western blot both showed that WISP1 expressions in GC cell lines were significantly higher than that in GES-1 cell lines ($P < 0.01$, **Figure 2A**, **2B**). To down-regulated WISP1 expression, siWISP1 was constructed and then transfected into GC cell lines BGC823 and SGC7901, and the transfection of siWISP1 successfully knockdown the WISP1 expression in GC cell lines (**Figure 2C**, **2D**). After transfection, CCK-8 assay and colony formation assay were respectively performed to measure the cell proliferation and cell colony formation. As shown as **Figure 2E**, **2F**, siWISP1 transfection obviously inhibited cell proliferation and colony numbers in BCG823 and SGC7901 cell lines ($P < 0.01$). The effects of WISP1 knockdown on GC cell apoptosis and cell cycle were both assessed using flow cytometry and the results showed that siWISP1 transfection notably promoted cell apoptosis and induced cell cycle arrest in G1 phase ($P < 0.01$, **Figure 2G**, **2H**). These results proved that the knockdown of WISP1 could suppress cell proliferation and colony formation as well as enhance cell cycle arrest and apoptosis in GC cell lines.

Knockdown of WISP1 inhibited the activity of AKT/mTOR pathway signaling pathway in GC cells

To further investigate the impacts of WISP1 in GC, the expression levels of proliferation-related factors (PCNA and Cyclin D1) and apoptosis-related factors (caspase-3, cleaved-caspase-3, Bcl-2, Bax and p53) in BCG BCG823 and SGC7901 cell lines that transfected with siWISP1 or siNC were detected using western blot. Results of western blot showed that WISP1 knockdown significantly decreased the expressions of PCNA, Cyclin D1 and Bcl-2 and increased the expressions of cleaved-caspase-3, caspase-3, Bax and p53 compared with siNC group ($P < 0.01$, **Figure 3A**). Then, we assumed that WISP1 affected GC development through regulating AKT/mTOR signaling pathway according to previous studies [20, 21]. To

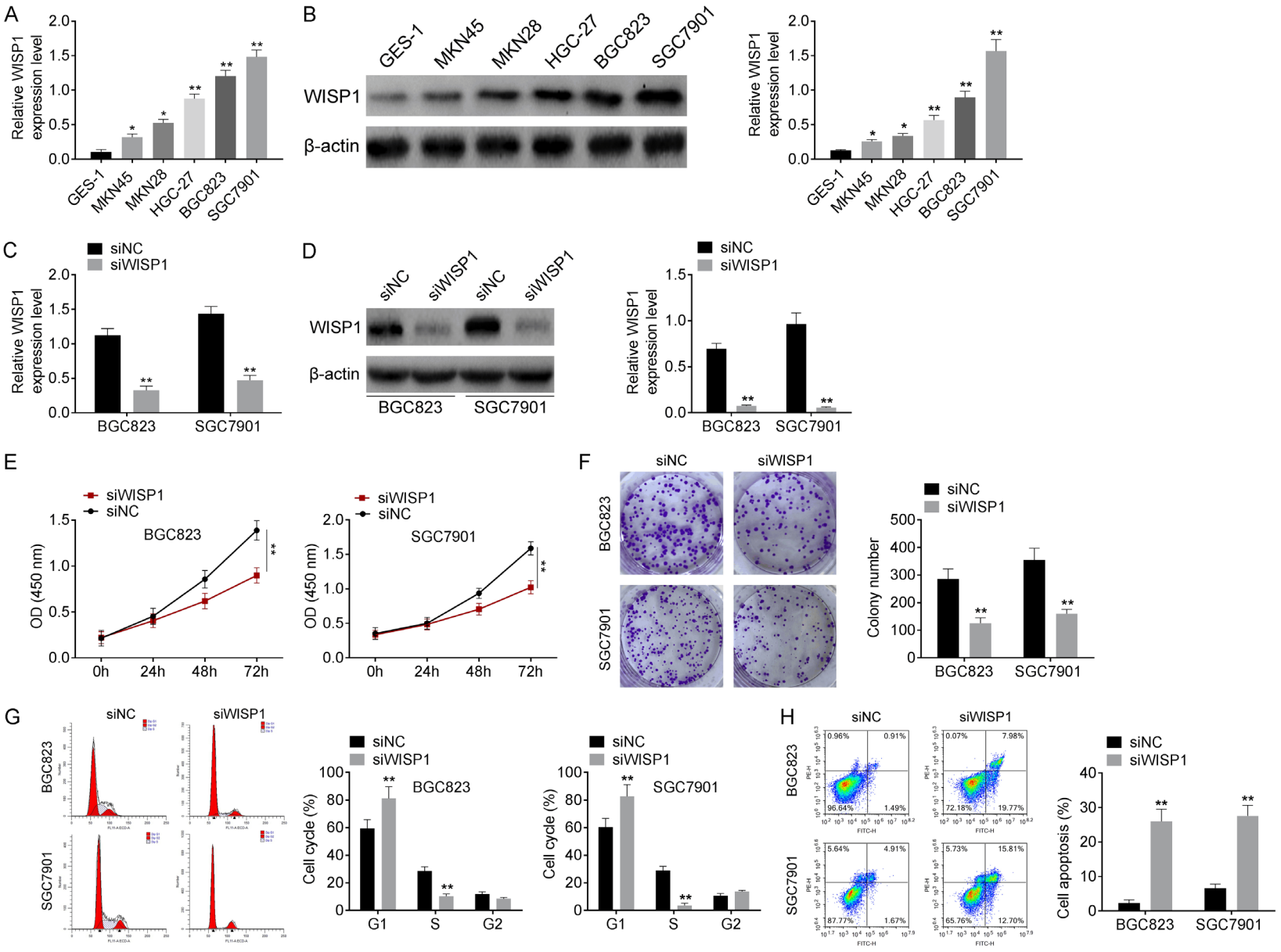

Figure 2. Knockdown of WISP1 inhibited cell proliferation and colony formation, interdicted cell cycle and promoted cell apoptosis in GC. The expression levels of human normal gastric mucosal epithelial cell GES-1 and GC cell lines including MKN45, MKN28, HGC-27, BGC823 and SGC7901 were detected using (A) qRT-PCR

and (B) western blot. GC cell lines BGC823 and SGC7901 were transfected with siWISP1 or siNC, the transfection efficiency was measured using (C) qRT-PCR and (D) western blot. (E) After transfection, the cell proliferation was analyzed using CCK-8 assay. (F) The colony cell number was assessed using cell colony formation assay. (G) The cell cycle and (H) apoptosis were determined using flow cytometry. Data were shown as mean ± SD. *$P < 0.05$, **$P < 0.01$ vs siNC groups.

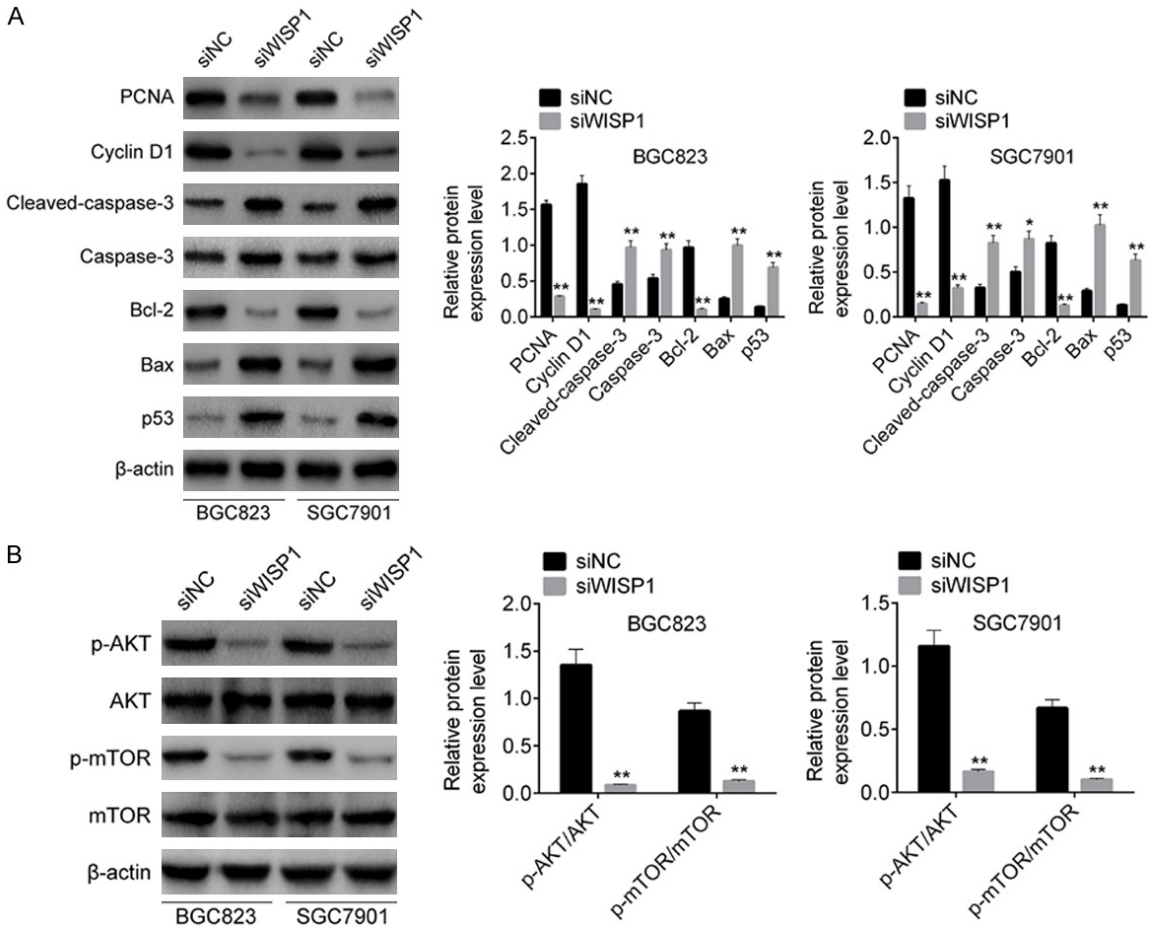

Figure 3. Knockdown of WISP1 inhibited the activity of AKT/mTOR pathway signaling pathway in GC cells. A. The protein expression levels of PCNA, Cyclin D1, cleaved-caspase-3, caspase-3, Bcl-2, Bax and p53 in GC cell lines BGC823 and SGC7901 that were transfected with siWISP1/siNC were detected using western blot. B. The protein expression levels of p-AKT/AKT and p-mTOR/mTOR in GC cell lines BGC823 and SGC7901 that were transfected with siWISP1/siNC were measured using western blot. β-actin was served as the normalized protein. Data were shown as mean ± SD. *$P < 0.05$, **$P < 0.01$ vs siNC groups.

verify the assumption, the expressions of AKT/mTOR related proteins, including p-AKT/AKT and p-mTOR/mTOR, were measured using western blot. As shown as **Figure 3B**, the expression levels of p-AKT/AKT and p-mTOR/mTOR were both memorably down-regulated in siWISP1 group when compared to that in siNC group ($P < 0.01$). These data confirmed that the silence of WISP1 inhibited proliferation, promoted apoptosis and inactivated AKT/mTOR signaling pathway.

Knockdown of WISP1 acted on GC cell activities via regulating AKT/mTOR signaling pathway

To further explore the molecular mechanism of WISP1 in GC, GC cell line BGC823 was transfected with AKT inhibitor LY294002 and/or siWISP1, and the BGC823 cell lines were subsequently divided into three groups: siNC, siWISP1 and siWISP1 + LY294002 groups. Then, the cell proliferation, colony formation,

cell cycle were apoptosis detected. CCK-8 assay showed that LY294002 treatment significantly restored the decrease of cell proliferation that induced by siWISP1 transfection ($P < 0.01$, **Figure 4A**). Next, data from colony formation assay exhibited that the colony cell number of siWISP1 + LY294002 group was remarkably more than that of siWISP1 group ($P < 0.01$, **Figure 4B**). Moreover, results of flow cytometry revealed that LY294002 treatment could markedly relieved the cell cycle arrest and cell apoptosis that induced by siWISP1 transfection ($P < 0.01$, **Figure 4C**, **4D**). In addition, the expression levels of PCNA, Cyclin D1, cleaved-caspase-3, caspase-3, Bcl-2, Bax and p53 were monitored using western blot and the results of western blot was shown as **Figure 4E**. Obviously, LY29004 could regain the decreases of PCNA, Cyclin D1 and Bcl-2 expressions and the increases of cleaved-caspase-3, caspase-3, Bax and p53 expressions which were induced by siWISP1 transfection ($P < 0.01$). These results suggested that the effects of WISP1 knockdown on GC cell proliferation, colony formation, cell cycle and apoptosis were eliminated when the AKT/mTOR signaling pathway was blocked.

Knockdown of WISP1 inhibited GC tumor growth and accelerated tumor apoptosis in vivo

To examine the influences of WISP1 on GC *in vivo*, nude mice were used to establish GC animal models. BGC823 cell lines that transfected with shWISP1 or shNC were injected into nude mice and the mice were subsequently divided into shNC group and shWISP1 group. As shown as **Figure 5A-C**, the tumor volumes, sizes and weights of mice in shWISP1 groups were all significantly less than that in shNC group ($P < 0.01$). IHC assay showed that the expressions of Ki-67 and WISP1 were both notably decreased in shWISP1 group when compared to shNC group ($P < 0.01$, **Figure 5D**). Furthermore, images from TUNEL assay revealed that the TUNEL-positive cells in shNC group were markedly more than that in shWISP1 group ($P < 0.01$, **Figure 5E**). Then, the expressions of p-AKT/AKT and p-mTOR/mTOR in the mice tumor tissues were detected using western blot. As shown as **Figure 5F**, the p-AKT/AKT and p-mTOR/mTOR expressions were both significantly inhibited in shWISP1 group when compared to that in shNC group ($P < 0.01$). Above results illustrated that the knockdown of WISP1 could repress GC tumor growth and proliferation and facilitate tumor apoptosis *in vivo*.

Discussion

GC is one of the most common cancers of the digestive tract worldwide with a high morbidity and mortality [1]. In recent years, a large number of researches on the pathogenesis of GC show that the development of GC is a complex pathophysiological process involving multiple factors, procedures and pathways. A variety of carcinogenic factors, tumor suppressor factors and inflammatory mediators are implicated in the GC occurrence [22]. Therefore, in-depth study of the pathogenesis and development of GC is of great significance for improving the early diagnosis rate and clinical prognosis of GC patients. Many scholars have reported various biomarkers that could act on GC. Brasacchio et al. [23] reported that p300/CBP-associated protein (PCAF)/adaptor protein 3 (ADA3) acted as a tumor inhibitor and effected on the process of premalignant to malignant change in GC via the mitochondrial pathway. Kanda et al. [24] found that synaptotagmin VIII (SYT8) was overexpressed in GC tissues and its high expression was related to peritoneal metastasis, and they also proved that SYT8 might be a prognostic biomarker in GC therapy. Zhang et al. [25] confirmed that lncRNA HOXC-AS3 played as a oncogene in GC and indicated poor prognosis, and it could modulate the occurrence and progression of GC via targeting YBX1. However, people's understanding of biomarkers is still limited, and the functions of various genes that affect GC need to be explored.

WISP1 was reported as a carcinogenic gene in many cancers. Lee et al. [26] reported that WISP1 indicated high risk of urothelial cell carcinoma development and its expression was related to large tumor size and invasive tumor of urothelial cell carcinoma. Deng et al. [27] found that WISP1 could induce metastasis and invasion in melanoma via enhancing the epithelial-mesenchymal transition. Chang et al. [28] proved that WISP1 negatively regulated miR-153-3p expression and activated Snail and FAK/ILK/AKT signaling pathways in oral squamous cell carcinoma. However, the role of WISP1 played in GC has not been reported.

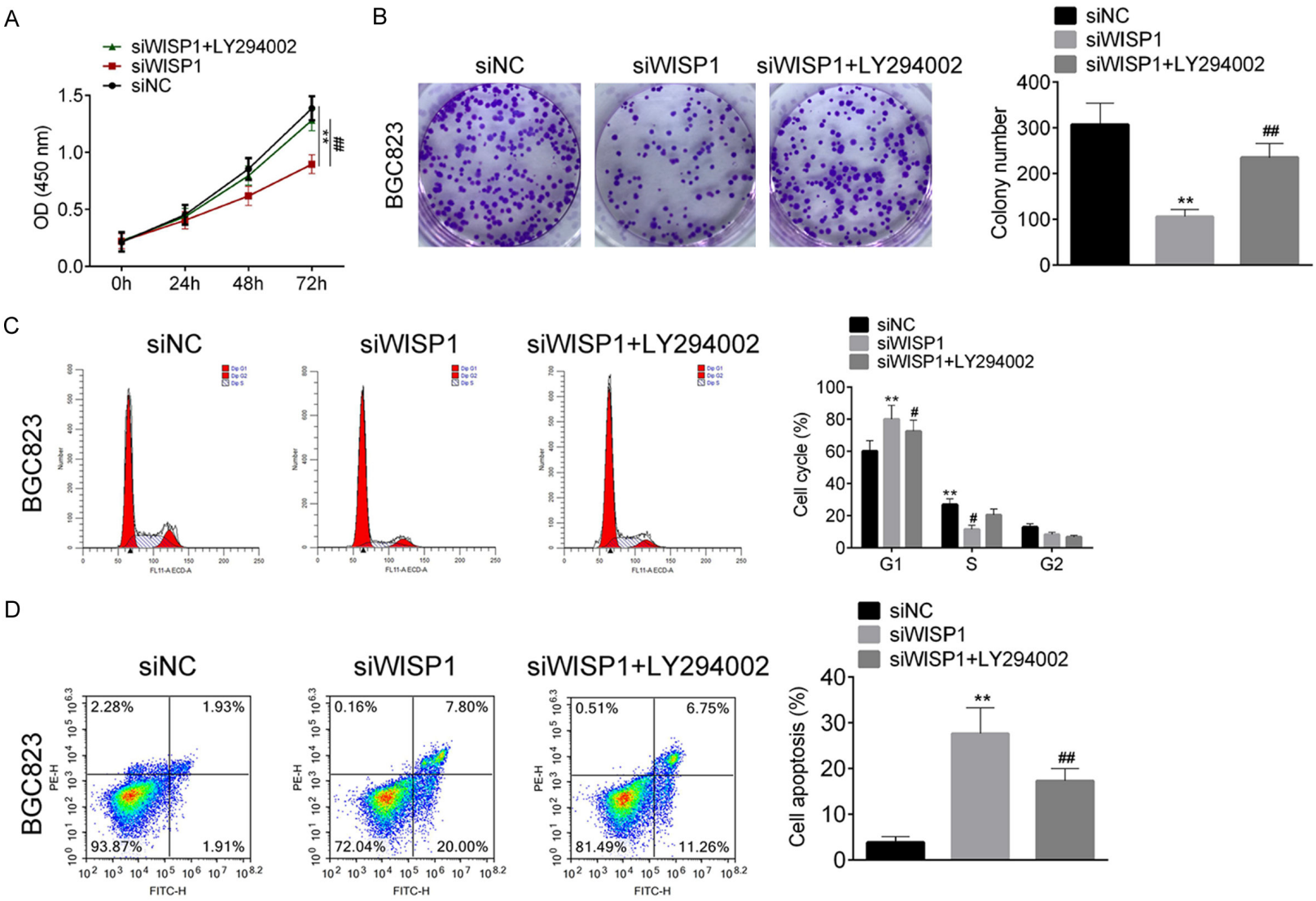
A
siWISP1+LY294002
siWISP1
siNC
OD (450 nm)
1.5
1.0
0.5
0.0
0h
24h
48h
72h
**
##
B
siNC
siWISP1
siWISP1+LY294002
BGC823
Colony number
400
300
200
100
0
C
siNC
siWISP1
siWISP1+LY294002
BGC823
Cell cycle (%)
100
80
60
40
20
0
G1
S
G2
D
siNC
siWISP1
siWISP1+LY294002
BGC823
2.28%
1.93%
93.87%
1.91%
0.16%
7.80%
72.04%
20.00%
0.51%
6.75%
81.49%
11.26%
PE-H
FITC-H
Cell apoptosis (%)
40
30
20
10
0

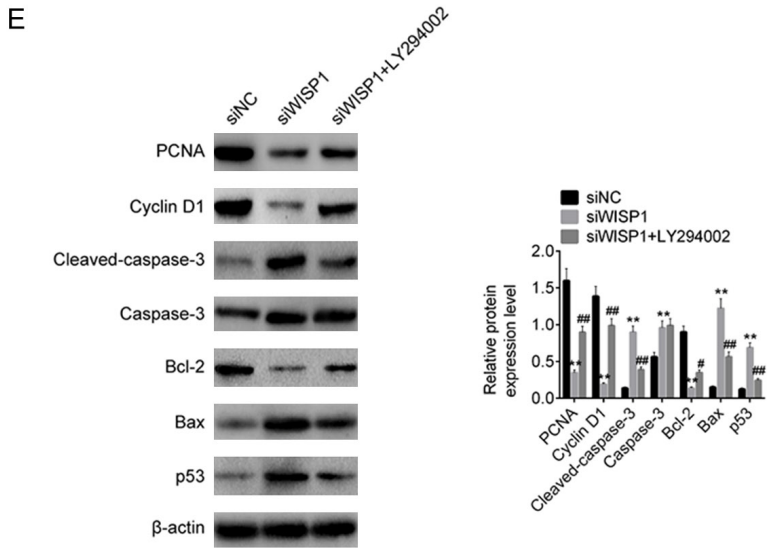

Figure 4. Knockdown of WISP1 modulated GC cell activities via regulating AKT/mTOR signaling pathway. GC cell lines BGC823 were divided into three groups, including siNC group, siWISP1 group and siWISP1 + LY294002 group. (A) The cell proliferation was detected using qRT-PCR. (B) The colony cell number was measured using cell colony formation assay. (C) The cell cycle and (D) apoptosis were determined using flow cytometry. (E) The protein expression levels of PCNA, Cyclin D1, cleaved-caspase-3, caspase-3, Bcl-2, Bax and p53 were monitored using western blot. β-actin was served as the normalized protein. Data were shown as mean ± SD. $^{**}P < 0.01$ vs siNC group, $^{\#}P < 0.05$ vs siWISP1group, $^{\#\#}P < 0.01$ vs siWISP1 group.

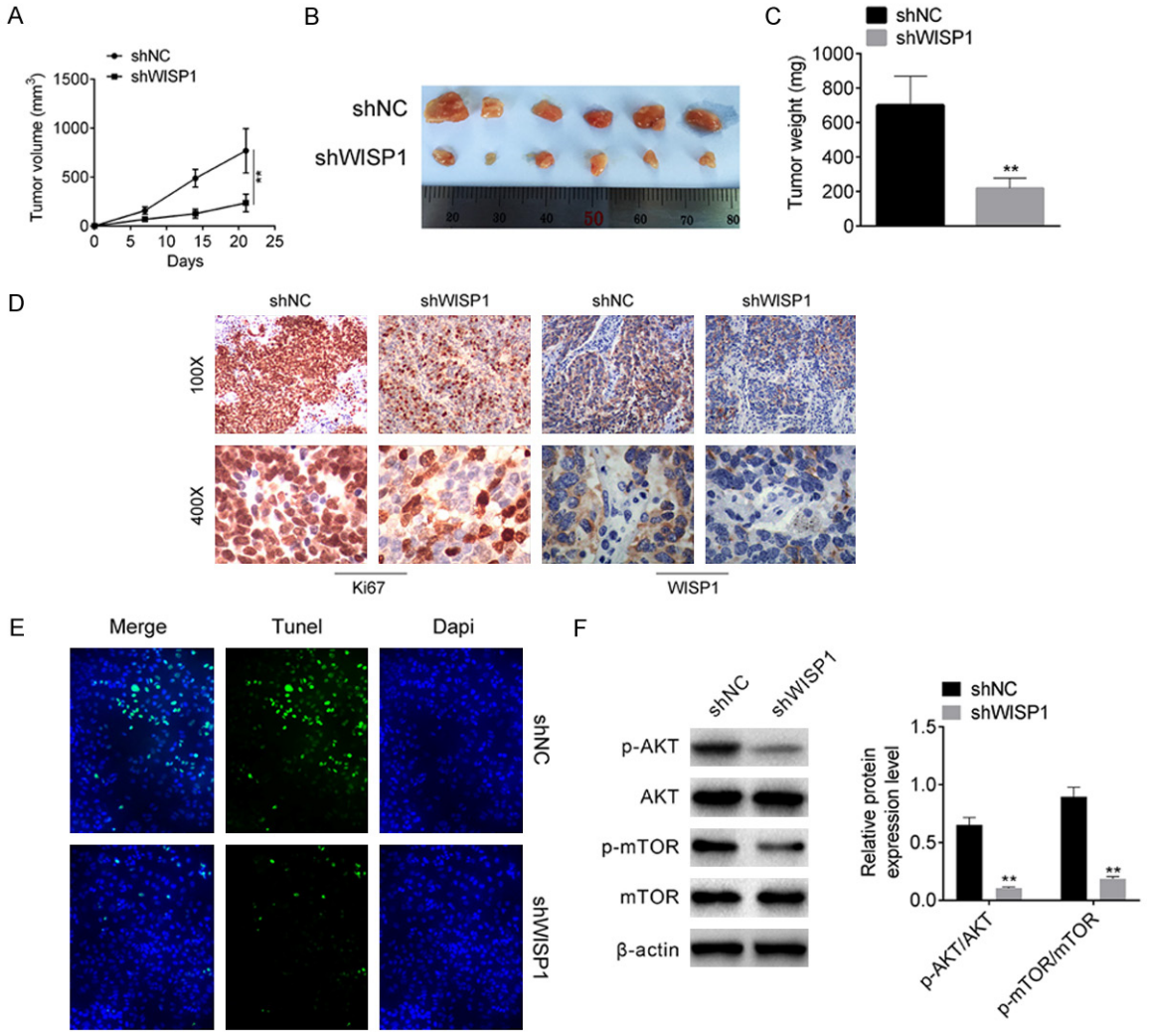

Figure 5. Knockdown of WISP1 inhibited GC tumor growth and accelerated tumor apoptosis *in vivo*. (A) The tumor volumes of GC mice models were measured weekly after injection. (B) The tumor sizes and (C) weights of GC mice models were monitored after the mice were killed. (D) The expression level of Ki-67 and WISP1 were detected using IHC. (E) The apoptotic cells in mice GC tumor tissues were assessed using TUNEL assay. Data were shown as mean ± SD. (F) The expression levels of p-AKT/AKT and p-mTOR/mTOR were detected using western blot. $^{**}P < 0.01$ vs shNC group.

In the present study, we firstly found that WISP1 was highly expressed in GC tissues and cell lines and the over-expression of WISP1 was associated with the shorter survival rate and poor prognosis of GC patients. Then, the expressions of WISP1 in human GC cell lines BGC823 and SGC7901 were down-regulated through siWISP1 transfection. The cell proliferation and colony formation were respectively detected using CCK-8 assay and cell colony assay while the cell cycle and apoptosis were both measured using flow cytometry. Our results showed that the knockdown of WISP1 inhibited cell proliferation and colony formation, promoted cell apoptosis and induced cell cycle arrest in GC cell lines. PCNA [29] and Cyclin D1 [30] have been reported as the pro-proliferation factors. Cleaved-caspase-3, caspase-3, Bax and p53 were recognized as the pro-apoptosis factors while Bcl-2 was known as an anti-apoptosis factor [31]. To further define the effects of WISP1 on GC cells activities, the protein expressions of PCNA, Cyclin D1, cleaved-caspase-3, caspase-3, Bcl-2, Bax and p53 were determined using western blot. The results showed that siWISP1 transfection suppressed PCNA, Cyclin D1 and Bcl-2 expressions and enhanced cleaved-caspase-3, cas-

pase-3, Bax and p53 expressions in GC cell lines. It further proved that the knockdown of WISP1 inhibited cell proliferation and promoted cell apoptosis in GC cells.

Then, we predicted that WISP1 affected GC through AKT/mTOR signaling pathway based on previous studies [20, 21]. To verify the prediction, the expression levels of p-AKT/AKT and p-mTOR/mTOR of transfected GC cell lines were detecting using western blot. Data from western blot displayed that the knockdown of WISP1 significantly reduced the expressions of p-AKT/AKT and p-mTOR/mTOR in GC cell lines BGC823 and SGC7901. In addition, to further validate the prediction, the AKT signaling pathway was interdicted in BGC823 cell lines that transfected with siWISP1 by LY294002 treatment. We found that the decreases of cell proliferation and colony formation, the arrest of cell cycle and the increase of cell apoptosis, which were induced by siWISP1, were recovered when the cells were underwent LY294002 treatment. Besides, we also found that LY294002 treatment recovered the decreases of PCNA, Cyclin D1 and Bcl-2 expressions and the increases of cleaved-caspase-3, caspase-3, Bax and p53 expressions in GC cell lines which were induced by WISP1 knockdown. These results elucidated that WISP1 regulated GC cell activities through AKT/mTOR signaling pathway *in vitro*.

Furthermore, GC nude mice model was constructed to investigate the role of WISP1 played on GC tumor growth *in vivo*. We elucidated that the tumor volumes, sizes and weights of shWISP1 group mice were all less than that in shNC groups. And, we found that the knockdown of WISP1 inhibited Ki-67 expression and increased TUNEL-positive cells *in vivo*. Besides, p-AKT/AKT and p-mTOR/mTOR expressions in tumor tissues of the two groups of mice were detected using western blot. Data from western blot exhibited that the down-regulation of WISP1 reduced the expression levels of p-AKT/AKT and p-mTOR/mTOR *in vivo*. These results illustrated that WISP1 knockdown could suppress tumor growth and proliferation and accelerated tumor apoptosis through AKT/mTOR signaling pathway *in vivo*.

In conclusion, the current study demonstrated that knockdown of WISP1 inhibited cell proliferation and colony formation, interdicted cell cycle and promoted cell apoptosis in GC via regulating AKT/mTOR signaling pathway *in vitro* and *in vivo*. These findings provided a novel insights and theoretical basis into the application of WISP1 in the GC therapy.

Disclosure of conflict of interest

None.

Address correspondence to: Dr. Wei Li, Department of Pediatrics, The First Affiliated Hospital of China Medical University, No. 155 Nanjing North Street, Shenyang 110001, China. Tel: +86-13889258356; E-mail: drliwei225@163.com

References

[1] Bray F, Ferlay J, Soerjomataram I, Siegel RL, Torre LA and Jemal A. Global cancer statistics 2018: GLOBOCAN estimates of incidence and mortality worldwide for 36 cancers in 185 countries. CA Cancer J Clin 2018; 68: 394-424.

[2] Balakrishnan M, George R, Sharma A and Graham DY. Changing trends in stomach cancer throughout the world. Curr Gastroenterol Rep 2017; 19: 36.

[3] Siegel RL, Miller KD and Jemal A. Cancer statistics, 2019. CA Cancer J Clin 2019; 69: 7-34.

[4] Montori G, Coccolini F, Fugazzola P, Ceresoli M, Tomasoni M, Rubicondo C, Raimondo S, Pinelli D, Colledan M and Frigerio L. Cytoreductive surgery and hyperthermic intraperitoneal chemotherapy in ovarian and gastrointestinal peritoneal carcinomatosis: results from a 7-year experience. J Gastrointest Oncol 2018; 9: 241.

[5] Coburn N, Cosby R, Klein L, Knight G, Malthaner R, Mamazza J, Mercer CD and Ringash J. Staging and surgical approaches in gastric cancer: a systematic review. Cancer Treat Rev 2018; 63: 104-115.

[6] Sitarz R, Skierucha M, Mielko J, Offerhaus GJA, Maciejewski R and Polkowski WP. Gastric cancer: epidemiology, prevention, classification, and treatment. Cancer Manag Res 2018; 10: 239.

[7] Kim ST, Cristescu R, Bass AJ, Kim KM, Odegaard JI, Kim K, Liu XQ, Sher X, Jung H, Lee M, Lee S, Park AH, Park JO, Park YS, Lim HY, Lee H, Choi M, Talasaz A, Kang P, Cheng J, Loboda A, Lee J and Kang WK. Comprehensive molecular characterization of clinical responses to PD-1 inhibition in metastatic gastric cancer. Nat Med 2018; 24: 1449.

[8] Ge S, Xia X, Ding C, Zhen B, Zhou Q, Feng J, Yuan J, Chen R, Li Y, Ge Z, Ji J, Zhang L, Wang J, Li Z, Lai Y, Hu Y, Li Y, Li Y, Gao J, Chen L, Xu J, Zhang C, Jung SY, Choi JM, Jain A, Liu M, Song L, Liu W, Guo G, Gong T, Huang Y, Qiu Y, Huang

W, Shi T, Zhu W, Wang Y, He F, Shen L and Qin J. A proteomic landscape of diffuse-type gastric cancer. Nature Commun 2018; 9: 1012.
[9] Yang H, Zhang H, Ge S, Ning T, Bai M, Li J, Li S, Sun W, Deng T, Zhang L, Ying G and Ba Y. Exosome-derived miR-130a activates angiogenesis in gastric Cancer by targeting C-MYB in vascular endothelial cells. Mol Ther 2018; 26: 2466-2475.
[10] Jeong MH, Park SY, Lee SH, Seo J, Yoo JY, Park SH, Kim MJ, Lee S, Jang S, Choi HK, Lee JE, Shin SJ, Choi KC, Cheong JH and Yoon HG. EPB41L5 mediates TGFβ-induced metastasis of gastric cancer. Clin Cancer Res 2019; 25: 3617-3629.
[11] Zhao R, Zhang Y, Zhang X, Yang Y, Zheng X, Li X, Liu Y and Zhang Y. Exosomal long noncoding RNA HOTTIP as potential novel diagnostic and prognostic biomarker test for gastric cancer. Mol Cancer 2018; 17: 68.
[12] Tacke C, Aleksandrova K, Rehfeldt M, Murahovschi V, Markova M, Kemper M, Hornemann S, Kaiser U, Honig C, Gerbracht C, Kabisch S, Hörbelt T, Ouwens DM, Weickert MO, Boeing H, Pfeiffer AFH, Pivovarova O and Rudovich N. Assessment of circulating Wnt1 inducible signalling pathway protein 1 (WISP-1)/CCN4 as a novel biomarker of obesity. J Cell Commun Signal 2018; 12: 539-548.
[13] Deng W, Fernandez A, McLaughlin SL and Klinke DJ 2nd. WNT1 inducible signaling pathway protein 1 (WISP1) stimulates melanoma cell invasion and metastasis by promoting epithelial-mesenchymal transition (EMT). J Biol Chem 2019; 294: 5261-5280.
[14] Hashimoto Y, Shindookada N, Tani M, Nagamachi Y, Takeuchi K, Shiroishi T, Toma H and Yokota J. Expression of the Elm1 gene, a novel gene of the CCN (connective tissue growth factor, Cyr61/Cef10, and neuroblastoma overexpressed gene) family, suppresses in vivo tumor growth and metastasis of K-1735 murine melanoma cells. J Exp Med 1998; 187: 289-96.
[15] Maiese K. Novel applications of trophic factors, Wnt and WISP for neuronal repair and regeneration in metabolic disease. Neural Regen Res 2015; 10: 518-528.
[16] Klee S, Lehmann M, Wagner D, Baarsma HA and Königshoff M. WISP1 mediates IL-6-dependent proliferation in primary human lung fibroblasts. Sci Rep 2016; 6: 20547.
[17] Chang AC, Chen PC, Lin YF, Su CM, Liu JF, Lin TH, Chuang SM and Tang CH. Osteoblast-secreted WISP-1 promotes adherence of prostate cancer cells to bone via the VCAM-1/integrin α4β1 system. Cancer Lett 2018; 426: 47-56.
[18] Wang L, Sun J and Cao H. MicroRNA-384 regulates cell proliferation and apoptosis through directly targeting WISP1 in laryngeal cancer. J Cell Biochem 2019; 120: 3018-3026.
[19] Wang Y, Yang SH, Hsu PW, Chien SY, Wang CQ, Su CM, Dong XF, Zhao YM and Tang CH. Impact of WNT1-inducible signaling pathway protein-1 (WISP-1) genetic polymorphisms and clinical aspects of breast cancer. Medicine 2019; 98: e17854.
[20] Lu S, Liu H, Lu L, Wan H, Lin Z, Qian K, Yao X, Chen Q, Liu W, Yan J and Liu Z. WISP1 overexpression promotes proliferation and migration of human vascular smooth muscle cells via AKT signaling pathway. Eur J Pharmacol 2016; 788: 90-97.
[21] Shang Y, Chong Z, Wang S and Maiese K. Wnt1 inducible signaling pathway protein 1 (WISP1) targets PRAS40 to govern β-amyloid apoptotic injury of microglia. Curr Neurovasc Res 2012; 9: 239-249.
[22] Akyala AI and Peppelenbosch MP. Gastric cancer and Hedgehog signaling pathway: emerging new paradigms. Genes Cancer 2018; 9: 1.
[23] Brasacchio D, Busuttil RA, Noori T, Johnstone RW, Boussioutas A and Trapani JA. Down-regulation of a pro-apoptotic pathway regulated by PCAF/ADA3 in early stage gastric cancer. Cell Death Dis 2018; 9: 442.
[24] Kanda M, Shimizu D, Tanaka H, Tanaka C, Kobayashi D, Hayashi M, Iwata N, Niwa Y, Yamada S, Fujii T, Sugimoto H, Murotani K, Fujiwara M and Kodera Y. Significance of SYT8 for the detection, prediction, and treatment of peritoneal metastasis from gastric cancer. Ann Surg 2018; 267: 495-503.
[25] Zhang E, He X, Zhang C, Su J, Lu X, Si X, Chen J, Yin D, Han L and De W. A novel long noncoding RNA HOXC-AS3 mediates tumorigenesis of gastric cancer by binding to YBX1. Genome Biol 2018; 19: 154.
[26] Lee HL, Chiou HL, Wang SS, Hung SC, Chou MC, Yang SF, Hsieh MJ and Chou YE. WISP1 genetic variants as predictors of tumor development with urothelial cell carcinoma. Urol Oncol 2018; 36: 160.
[27] Deng W, Fernandez A, McLaughlin SL and Klinke DJ 2nd. WNT1-inducible signaling pathway protein 1 (WISP1/CCN4) stimulates melanoma invasion and metastasis by promoting the epithelial-mesenchymal transition. J Biol Chem 2019; 294: 5261-5280.
[28] Chang AC, Lien MY, Tsai MH, Hua CH and Tang CH. WISP-1 promotes epithelial-mesenchymal transition in oral squamous cell carcinoma cells via the miR-153-3p/Snail Axis. Cancers 2019; 11: 1903.
[29] Jurikova M, Danihel Ľ, Polák Š and Varga I. Ki67, PCNA, and MCM proteins: markers of

proliferation in the diagnosis of breast cancer. Acta Histochem 2016; 118: 544-552.
[30] Xia B, Yang S, Liu T and Lou G. miR-211 suppresses epithelial ovarian cancer proliferation and cell-cycle progression by targeting Cyclin D1 and CDK6. Mol Cancer 2015; 14: 57.
[31] Dolka I, Król M and Sapierzyński R. Evaluation of apoptosis-associated protein (Bcl-2, Bax, cleaved caspase-3 and p53) expression in canine mammary tumors: an immunohistochemical and prognostic study. Res Vet Sci 2016; 105: 124-133.